You might find this additional information useful...

Supplemental material for this article can be found at:
http://ajplung.physiology.org/cgi/content/full/00062.2007/DC1

This article cites 75 articles, 32 of which you can access free at:
http://ajplung.physiology.org/cgi/content/full/294/1/L79#BIBL

Updated information and services including high-resolution figures, can be found at:
http://ajplung.physiology.org/cgi/content/full/294/1/L79

Additional material and information about *AJP - Lung Cellular and Molecular Physiology* can be found
at:
http://www.the-aps.org/publications/ajplung

This information is current as of October 29, 2010 .

Effects of dynamic compression on lentiviral transduction in an in vitro airway wall model

Alice A. Tomei,[1] Melanie M. Choe,[2] and Melody A. Swartz[1,2]

[1]*Institute of Bioengineering, École Polytechnique Fédérale de Lausanne (EPFL), Lausanne, Switzerland; and* [2]*Department of Biomedical Engineering, Northwestern University, Evanston, Illinois*

Tomei AA, Choe MM, Swartz MA. Effects of dynamic compression on lentiviral transduction in an in vitro airway wall model. *Am J Physiol Lung Cell Mol Physiol* 294: L79–L86, 2008. First published November 16, 2007; doi:10.1152/ajplung.00062.2007.—Asthmatic patients are more susceptible to viral infection, and we asked whether dynamic strain on the airway wall (such as that associated with bronchoconstriction) would influence the rate of viral infection of the epithelial and subepithelial cells. To address this, we characterized the barrier function of a three-dimensional culture model of the bronchial airway wall mucosa, modified the culture conditions for optimization of ciliogenesis, and compared epithelial and subepithelial green fluorescent protein (GFP) transduction by a pWpts-GFP lentivirus, pseudotyped with VSV-G, under static vs. dynamic conditions. The model consisted of human lung fibroblasts, bronchial epithelial cells, and a type I collagen matrix, and after 21 days of culture at air liquid interface, it exhibited a pseudostratified epithelium comprised of basal cells, mucus-secreting cells, and ciliated columnar cells with beating cilia. Microparticle tracking revealed partial coordination of mucociliary transport among groups of cells. Slow dynamic compression of the airway wall model (15% strain at 0.1 Hz over 3 days) substantially enhanced GFP transduction of epithelial cells and underlying fibroblasts. Fibroblast-only controls showed a similar degree of transduction enhancement when undergoing dynamic strain, suggesting enhanced transport through the matrix. Tight junction loss in the epithelium after mechanical stress was observed by immunostaining. We conclude that dynamic compressive strain such as that associated with bronchoconstriction may promote transepithelial transport and enhance viral transgene delivery to epithelial and subepithelial cells. This finding has significance for asthma pathophysiology as well as for designing delivery strategies of viral gene therapies to the airways.

mechanical stress; three-dimensional model; asthma; bronchoconstriction; ciliogenesis; human

ASTHMA AND AIRWAY SUSCEPTIBILITY to viral infections have long been correlated clinically (2, 9, 16, 26, 36, 61, 62). Asthma is associated with recruitment of inflammatory cells, remodeling and thickening of the reticular basement membrane, subepithelial fibrosis, and airway smooth muscle hyperresponsiveness and hyperreactivity (reviewed in Refs. 7, 17, 19, 21, 23, 25, 48, 70). The epithelial barrier function of asthmatic airways is often damaged (35), possibly increasing susceptibility to viral infection. Moreover, it has been shown that epithelial cells from asthmatic patients express a higher number of viral receptors on their surface (4, 62), which when activated exacerbate epithelial secretion of cytokines like granulocyte-macrophage colony-stimulating factor, interleukin (IL)-6, IL-8, IL-11, and RANTES that help maintain a persistent inflammatory state (46).

Nevertheless, inflammatory mediators are only part of the story, as treatment with corticosteroids cannot cure asthma or reverse airway dysfunction or remodeling (16, 33). In particular, several different in vitro models of the bronchial airway wall have been used to demonstrate that mechanical stress, at levels relevant to bronchoconstriction, can itself induce changes in gene and protein expression in epithelial cells and fibroblasts that are consistent with airway wall remodeling events, as well as matrix remodeling and smooth muscle cell (SMC) migration and proliferation (11, 12, 31, 42, 60, 66, 73).

Since asthmatic airways undergo mechanical stresses during bronchoconstriction, and because repeated bronchoconstriction can lead to substantial remodeling of the airway wall, it is possible that mechanical stress may alter the susceptibility of asthmatic airways to viral infection. Here we address the question of whether physiologically relevant mechanical stress such as that associated with bronchoconstriction could affect viral infection of airway cells in an in vitro tissue model of the bronchial wall.

To examine the effect of compressive mechanical stress on viral infection of the bronchial wall, we used a three-dimensional (3D) in vitro model of the airway wall using human bronchial epithelial cell-fibroblast coculture. Such a model has many advantages over animal models or cultured cells from human biopsies (28): in vitro models are well-defined, reproducible, and controllable; they can use human cells, and importantly, the role of mechanical stress can be isolated from that of inflammation. Of course, to be able to draw physiologically relevant conclusions from an in vitro model of viral infection in the airway wall, the model must exhibit a functionally relevant epithelial barrier. In vivo, the barrier function of the epithelium is comprised of a mucus layer, a dense carpet of beating cilia, a pseudostratified epithelial layer with tight cell-cell junctions, and the basement membrane, which is secreted and maintained by the basal epithelium and serves as an important barrier function between the epithelial and mesenchymal cells (Fig. 1A). During normal breathing, the bronchial wall undergoes negligible circumferential strain (14). Compressive stress in the bronchial airways occurs when smooth muscle shortens, making the airway constrict; this can occur, for example, during breath-holding, and frequently occurs in asthma. The stress and strain profiles in the airway wall during bronchoconstriction are highly nonuniform, particularly with regards to the epithelium, which buckles to maintain
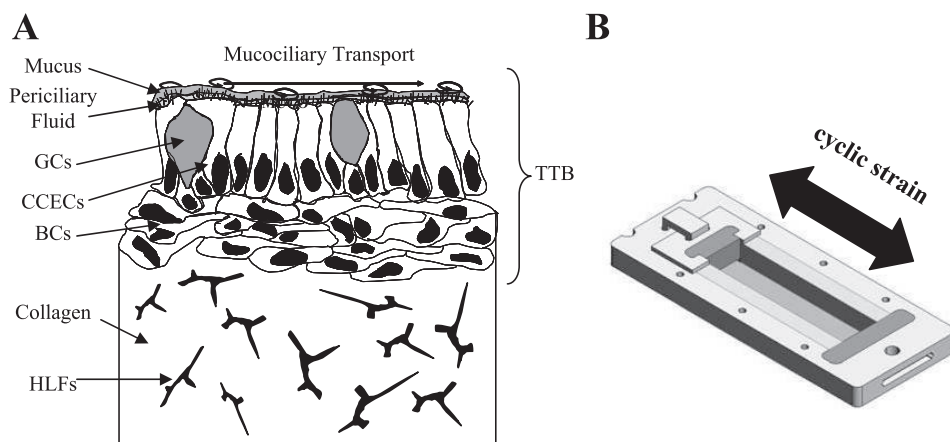
Fig. 1. Airway wall coculture model and strain device. *A*: schematic of the coculture model showing features relevant to the barrier function of the epithelium. HLFs, human fetal lung fibroblasts; TTB, transepithelial transport barrier; CCECs, ciliated columnar epithelial cells; BCs, basal cells; GCs, goblet cells. A lower viscosity periciliary fluid covers the basal part of the cilia while a more viscous mucus layer covers the apical part. The whip-like motion of the cilia propels the mucus in a well-defined direction. *B*: schematic of the strain device in which the airway wall model is cultured to a differentiated state, and then cyclic compression is applied for 72 h. In a Teflon frame, the collagen matrix is constrained on the two shorter sides by porous polyethylene (PE) and on the two longer sides by porous elastic sponge glued to the PE with silicon glue. One PE side is fixed to the frame while the other is mounted on a Teflon insert designed to slide along the walls of the frame to compress or stretch the collagen matrix. In static conditions, this side is anchored by a Teflon hook. On the bottom of the frame is a porous polycarbonate membrane to allow nutrient exchange between the model and the medium underneath.

constant perimeter (40, 41, 58, 74). In asthma, bronchoconstriction occurs more frequently, due to hyperresponsive SMCs (24, 25), and at greater magnitude, due to both hyperreactive SMCs and the remodeled airway wall (41, 57, 58, 74), which lead to fewer and deeper folds in the buckled epithelial layer in response to constriction.

Although in vitro airway wall models to mimic various features of the bronchial airways have been developed by ourselves and others (10–13, 20, 44, 50, 51, 64, 71), their degree of ciliogenesis, a critical barrier function, is often low. Using a 3D fibroblast-epithelial coculture model of the human airway wall mucosa that can undergo 3D lateral dynamic strain as would occur during bronchoconstriction (11), we first optimized culture conditions for key functional features, including a pseudostratified epithelium, mucus secretion, and an extensive carpet of beating cilia that display some degree of cell-to-cell synchrony. We then used this model to demonstrate that dynamic compressive strain substantially enhances viral transport and infection using a green fluorescent protein (GFP)-containing lentiviral vector. Our results demonstrate that mechanical stress associated with bronchoconstriction may promote viral transport to epithelial and subepithelial cells and thus exacerbate the susceptibility of the airway wall to viral infection.

MATERIALS AND METHODS

Cell culture. Human fetal lung fibroblasts (HLFs; IMR-90, ATCC, Manassas, VA) were expanded in αMEM (GIBCO) supplemented with 10% FBS (Invitrogen, Paisley, UK) and 1% penicillin-streptomycin-amphotericin (Invitrogen) and used at passage 16. Normal human bronchial epithelial cells (NHBE; Cambrex, Verviers, Belgium) were expanded in supplemented bronchial epithelial growth medium (Cambrex) supplemented with 1.5 μg/ml BSA (Invitrogen) and 15 ng/ml retinoic acid (Sigma), and used at passage 3.

Coculture medium composition was varied to optimize ciliogenesis based on previously published protocols (12, 45, 55). The final optimized coculture medium, used for all the data presented in this study (*medium A*) consisted of 50% DMEM (low glucose, Invitrogen),

50% bronchial epithelial basal medium, 200 μg/ml bovine pituitary extract (Pel-Freez Biologicals, Rogers, AR), 0.5 ng/ml human recombinant epidermal factor (Collaborative Research, Lexington, MA), 5 μg/ml hydrocortisone, 0.5 μg/ml epinepherine, 10 μg/ml transferrin, 5 μg/ml insulin, 30 ng/ml retinoic acid, 6.5 ng/ml triiodothyronine, 1.5 μg/ml BSA, 12 μg/ml calcium chloride, 30 ng/ml ethanolamine, 0.3 μg/ml phosphoethanolamine, 50 μg/ml gentamicin, and 50 ng/ml amphotericin-B (all from Sigma). For optimization, we varied the concentration of retinoic acid, bovine pituitary extract, calcium, ethanolamine, phosphoethanolamine, and human recombinant epidermal factor and looked at ciliogenesis after 7, 14, and 21 days using scanning electron microscopy (see *Epithelial characterization*). For data presentation, we compared two of the different medium compositions tested and later refer to these as *medium A* (the optimal medium) and *medium B* (that used in our previous publications; Refs. 11, 12).

Airway wall model. The dynamic strain culture device (Fig. 1*B*) has been previously described (11). HLFs were suspended at 500,000 cells/ml in 2.5 mg/ml type I collagen (BD Biosciences, Basel, Switzerland) and allowed to polymerize at 37°C, 5% CO_2 within the culture device. The gel surface was then coated with a thin layer (~50 μl/cm²) of 2.5 mg/ml acellular collagen to serve as a scaffold for epithelial cell remodeling and secretion of the cells' own basement membrane, and after polymerization, the gel surface was covered with coculture medium. NHBEs were then seeded atop the collagen-HLF culture at 2,500 cells/mm² and allowed to attach for 2 h. Finally, the model was submerged in coculture medium for 7–9 days with medium changes every 2 days. The air liquid interface (ALI) was established after epithelial confluence was reached, and the model was maintained for up to 3 wk to allow epithelial differentiation into a pseudostratified layer. During medium changes, the epithelium was washed with 500 μl of HBSS (Invitrogen) and the lavage was stored at −80° for later detection of types I and III mucin.

Epithelial characterization. The model was characterized for relevant barrier function properties, including epithelial morphology, degree of differentiation and stratification, ciliogenesis and mucociliary transport, and mucus secretion. Samples were fixed and cryosectioned in 4% paraformaldehyde. Histological staining on 6-μm sections was used to determine overall morphology and to identify mucin-producing cells by Alcian blue (Sigma) and was imaged under an Olympus CX41 microscope with the Olympus DP12-2 camera. To label basal

epithelial cells, rabbit anti-human keratin 14 antibody (1:250, Covance, Berkeley, CA) and AlexaFluor 594-conjugated secondary IgG (1:500, Molecular Probes, Eugene, OR) were used on 10-μm-thick sections. AlexaFluor 488-conjugated phalloidin (1:50, Molecular Probes) was used to examine the actin cytoskeletal structure of columnar cells. Images were taken using a Zeiss Axiovert 200M fluorescence microscope and AxioCam MRm camera. Finally, tight junctions were visualized using a mouse anti-human occludin antibody (1 μg/ml, Zymed Laboratories, South San Francisco, CA) on 70-μm-thick sections and were imaged under a confocal microscope.

Scanning electron microscopy was used to characterize ciliogenesis after various times in ALI culture. Samples were fixed in 2% gluteraldehyde (Sigma) for 2 h, washed in Sorensen buffer solution, and treated with 1% osmium tethroxide for 1 h. Then, they were dehydrated in a sequence from 25 to 100% ethanol, dried by CO_2 critical point, coated with 20 nm of gold, and imaged with the Jeol JSM-6300F microscope equipped with the Mamiya 6×7 Joel UHR (TMX 120 ISO100) camera.

Protein dot blot was used to confirm mucin production as described previously (12). Briefly, samples and standards (mucin types I and III, Sigma) were filtered through a nitrocellulose membrane (NitroPure, GE Osmonics, Minnetonka, MN) using Bio-Dot SF apparatus (Bio-Rad, Hercules, CA). The membrane was stained with Alcian blue (for type III mucin) or periodic acid-Schiff (for type I mucin) and analyzed with the ChemiDoc XRS system (Bio-Rad).

To examine mucociliary transport function, fluorescent microspheres were tracked using long-exposure fluorescence microscopy. Without the surface being washed, 20 μl of 1-μm-diameter yellow-green polystyrene microspheres (4×10^7 particles/ml, FluoSphere, Molecular Probes) were gently pipetted onto the epithelial surface. After being allowed to settle for 2 h at 37°C and 5% CO_2 in a humidified environmental chamber on the microscope stage, the samples were observed. Images were taken at a 16-s exposure time and evaluated using ImageJ software (National Institutes of Health, Bethesda, MD), and the average velocity was calculated for each particle (total trajectory length/exposure time). Only particles that moved were chosen for calculations. In addition, AVI-format movies were created to verify the microsphere movements.

GFP lentivirus. Lentiviral vectors were produced via a transient expression system consisting of three genetic elements: a transfer construct (pWpts-GFP), a packaging construct (pCMVR8.74), and an envelope expression construct (pMD2.G); all were kind gifts of D. Trono. These expression constructs were maintained in the form of bacterial plasmids and were transfected into HEK293T cells to produce replication-defective lentivirus stocks. A volume of virus solution having a multiplicity of infection equal to 10 for the NHBE was diluted in 200 μl culture medium and pipetted onto the epithelial surface 1 h before the strain experiments were performed.

Strain application. The coculture model was created in a strain device that was recently developed in our laboratory (11; Fig. 1B). After 21 days of culture at ALI, a dynamic compression of 15% was imposed to the airway wall model at a frequency of 0.1 Hz for 72 h at constant strain rate (5-s compression followed by 5-s relaxation, both at 3% s^{-1}) inside a 5% CO_2, 37°C incubator by a linear motor connected to an electronic controller (Cosmos, Velmex, Bloomfield, NY).

Epithelial surface washes with HBSS and media changes were performed daily. After 72 h, the coculture models were fixed in 4% paraformaldehyde for 2 h and observed under a fluorescence microscope on the epithelial surface. The samples were then embedded in Tissue Tek, cryosectioned into thick (70 μm) sections, mounted in DAPI-containing mounting medium (Vectashield H-1200, Vectorlabs, Burlingame, CA), and imaged under a fluorescence microscope. ImageJ was used to analyze epithelial and subepithelial infection rates of the sections; both average intensity and total GFP-positive area were determined in at least 30 fields for each sample. Data were normalized to cell number (i.e., number of DAPI-positive nuclei per field). A Mann-Whitney *U*-test was used to compare static vs. strain data.
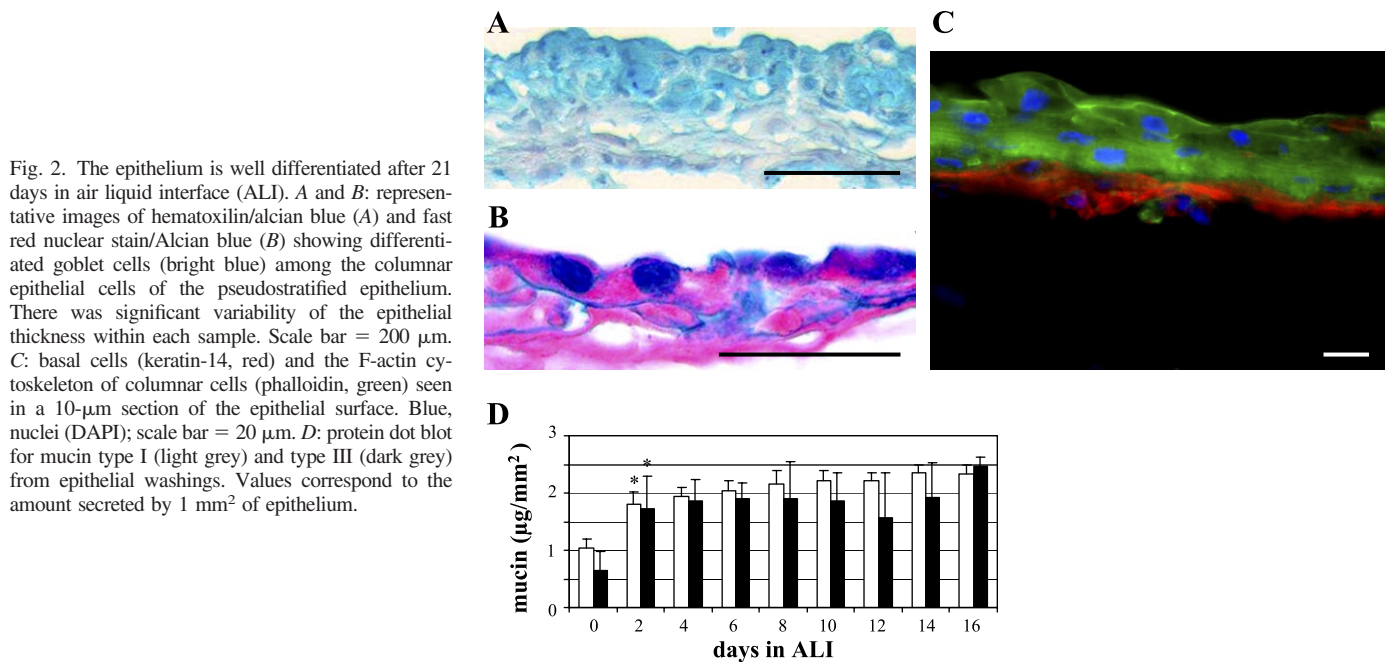
RESULTS

Epithelial morphology and mucin secretion. After 21 days in ALI, the epithelial surface achieved a pseudostratified morphology with well-differentiated epithelial cells including mucin-secreting cells, elongated basal cells, and ciliated columnar cells (Fig. 2). The mucin-secreting cells were present in a ratio of roughly 1:5. Mucin secretion was fairly consistent with time after 2 days in ALI (with average values of 2.13 ± 0.24 μg/mm^2 of epithelial surface area for type I mucin and 1.90 ± 0.80 μg/mm^2 for type III mucin).

Ciliogenesis and mucociliary transport. We first sought to optimize culture conditions for epithelial ciliogenesis. Compared with our previous work (11, 12), we found that the presence of calcium, ethanolamine, and phospho-ethanolamine as well as higher concentrations of retinoic acid (30 ng/ml) and bovine pituitary extract (200 μg/ml) improved the extent of ciliogenesis and cilia length (Fig. 3). In the optimal medium, the percent coverage of cilia was high (Fig. 3A), and the length of cilia (Fig. 3B) consistently reached 6–10 μm; both coverage and cilia length increased with time in ALI.

To evaluate cilia function and extent of coordination between neighboring cells, we tracked 1-μm fluorescent microspheres placed on the epithelial surface. Although we observed a large variability of mucociliary transport behavior between samples as well as within different regions of the same samples, we saw in many cases regions of coordinated motion (i.e., among groups of neighboring cells; Fig. 3E), as identified by long, parallel trajectories (arrows). The velocities of the particles were highly variable (Fig. 3F), and we observed many areas where microspheres moved in small circular patterns, indicating ciliary motion that is not coordinated between neighboring cells. (A short movie of the moving particles can be found in the online version of this article on the *AJP-Lung* web site.)

Lentivirus transport and infection in static vs. dynamic conditions. To determine whether dynamic strain affected viral infection rates of the epithelial and subepithelial cells, we used models that had been cultured for 21 days at ALI in the optimal medium and then exposed them for 72 h to either dynamic strain (15%, 0.1 Hz; dynamic) or no strain (control-static). We found that strain greatly enhanced the epithelial as well as subepithelial cell transduction of GFP by lentivirus (Fig. 4A). This was likely due to increased transport of the lentivirus as evidenced by the increased subepithelial depth at which fibroblasts were infected (Fig. 4A). Furthermore, we repeated the studies in epithelial-free (fibroblast-only) cultures and found a similar enhancement of infection with dynamic strain (Fig. 4, B–D), again indicating increased transport with strain.

Finally, to determine whether the barrier function of the epithelium was compromised by the dynamic strain, as has been reported to occur in vivo (35), we stained 70-μm-thick sections for occludin, a primary tight junctional protein in the epithelium. Because of the 3D nature of the model, we imaged these thick sections using confocal microscopy and saw that while epithelial cell-cell interfaces could be clearly delineated in static controls, dynamically compressed samples exhibited more diffuse and weaker staining, and cell-cell interfaces could not be delineated (Fig. 5A). Quantification of images revealed that the amount of occludin staining (% of occludin-positive area; Fig. 5B) was decreased in strained samples.

Fig. 2. The epithelium is well differentiated after 21 days in air liquid interface (ALI). *A* and *B*: representative images of hematoxilin/alcian blue (*A*) and fast red nuclear stain/Alcian blue (*B*) showing differentiated goblet cells (bright blue) among the columnar epithelial cells of the pseudostratified epithelium. There was significant variability of the epithelial thickness within each sample. Scale bar = 200 μm. *C*: basal cells (keratin-14, red) and the F-actin cytoskeleton of columnar cells (phalloidin, green) seen in a 10-μm section of the epithelial surface. Blue, nuclei (DAPI); scale bar = 20 μm. *D*: protein dot blot for mucin type I (light grey) and type III (dark grey) from epithelial washings. Values correspond to the amount secreted by 1 mm² of epithelium.

DISCUSSION

The incidence of asthma is continually increasing, and together with its secondary effects, which include increased susceptibility to viral infection (2, 9, 16, 22, 26, 36, 61), constitutes an enormous public health problem. Inflammatory cells and cytokines, bronchoconstriction, and airway wall remodeling all act synergistically to exacerbate the disease, and the enhanced epithelial susceptibility to viral pathogens and particulate matters also aggravates symptoms. It is likely that this increased susceptibility is at least partly caused by epithelial activation and damage and by factors including cytokines secreted by mesenchymal and inflammatory cells, which in turn cause loss of barrier function. However, asthmatic airways also experience compressive strain due to frequent brochocon-
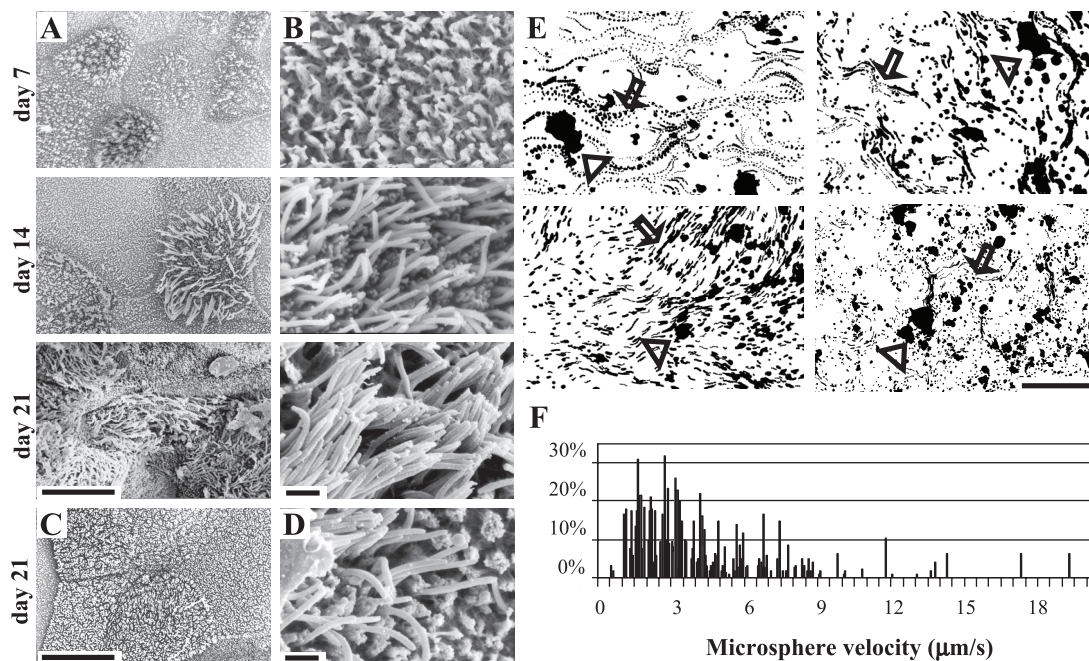

Fig. 3. Ciliogenesis and mucociliary function. *A* and *B*: scanning electron micrographs illustrate the extent of ciliogenesis at 7, 14, and 21 days of culture at ALI in the optimal medium composition *medium A*. Scale bars: *A* = 10 μm; *B* = 1 μm. *C* and *D*: micrographs of epithelial surface from less optimal *medium B*, used in previous studies (11, 12). Scale bars: *C* =10 μm; *D* =1 μm. All images in *A–D* are representative of cilia coverage within each sample. *E*: mucociliary transport as revealed by 16-s trajectories of 1-μm microspheres on the epithelium; 4 different experiments are shown to illustrate the range of variability seen. Regions of coordinated or synchronized ciliary movement can be identified by long, parallel trajectories (arrows), while small circular trajectories (arrowheads) indicate uncoupled ciliary movement from a single cell. Scale bar = 200 μm. *F*: distribution of average transport velocities of the microspheres. Only those microspheres that moved were included.
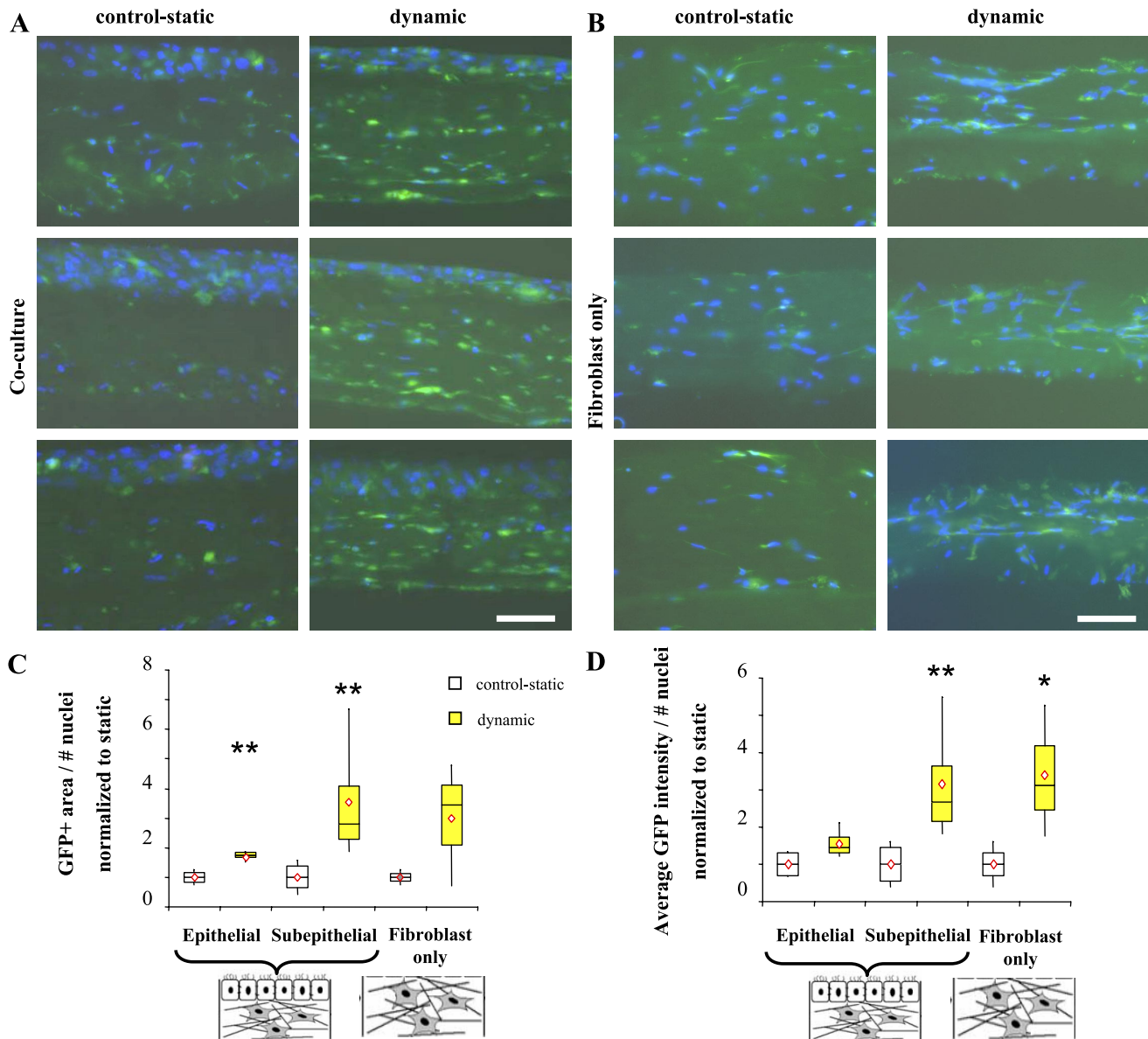
Fig. 4. VSV-G-lentiviral infection of airway wall cells under static vs. dynamic conditions. Infected cells (green) are revealed by their expression of green fluorescent protein (GFP) and nuclei are stained blue (DAPI). *A*: fluorescence micrographs of 80-μm sections of the airway wall model cultured in the strain device after 72 h of static (*left*) or dynamic strain (*right*) conditions. Scale bar = 100 μm. *B*: fluorescence micrographs of 80-μm sections of the fibroblast-only matrices again show increased infection under dynamic conditions. Scale bar = 100 μm. *C* and *D*: quantification of number of infected cells as expressed by GFP positive area per total cell number normalized to that in corresponding static controls (*C*) and amount of infection per cell as expressed by average GFP intensity per cell normalized to that in corresponding static controls (*D*). The interquartile range (box), full range (whiskers), mean (diamond), and median (line) are shown for each. *$P < 0.05$.

striction, and it has been demonstrated in vitro that mechanical compressive stress itself, at physiologically relevant levels, can activate the epithelium in asthmatic-like ways and induce airway wall remodeling events in the absence of inflammatory mediators (11, 12, 52, 60, 67, 68).

In this study, we showed that mechanical strain associated with bronchoconstriction, namely slow, dynamic lateral compression, can itself enhance viral infection of the cells in the airway mucosa. We suggest that such compressive strains are likely to increase transepithelial and subepithelial transport due to very small convective forces, as if squeezing a very dense sponge slowly. In turn, these small flows can drastically enhance transport of viruses, which are on the order of 100 nm

and thus have a Stokes-Einstein diffusivity of $\sim 6 \times 10^{-8}$ cm^2/s, and other large particles. In fact, even a very small dynamic strain of 15% at 0.1 Hz should drive fluid movement on the order of 600 μm/s, making the contribution of convection orders of magnitude greater than that of diffusion in overall transport from the apical surface towards the basal end of the model. In addition, our data suggest that dynamic compression may also decrease the barrier function of the epithelium by inducing partial loss of tight junctions. Our finding that such small stresses could, indeed, enhance viral infection rate may have important implications for designing strategies to delivering viral-based therapies to the airways, e.g., in the treatment of diseases such as cystic fibrosis.
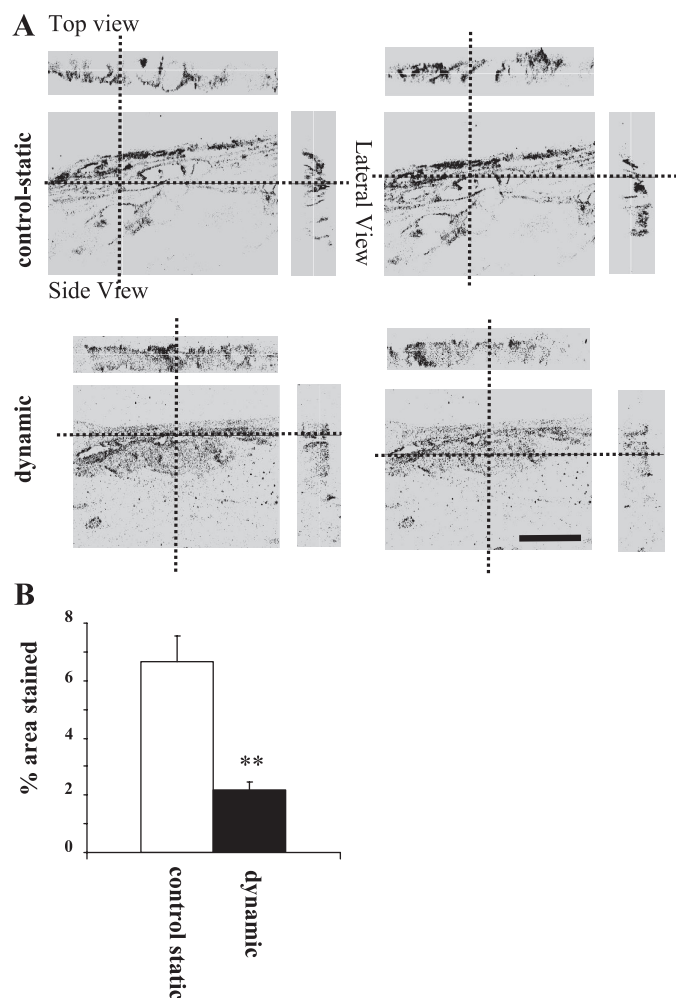
Fig. 5. Dynamic compression induces partial loss of tight junctions between epithelial cells. *A*: representative confocal micrographs (converted to grayscale and inverted) of 70-μm sections of the airway wall model cultured in the strain device after 72 h of control-static (*top*) or dynamic strain (*bottom*) conditions stained for occludin. Confocal slices through the *x* and *y* planes just along the epithelial cells show strong occludin staining that outlines epithelial cell borders in static conditions, while after dynamic strain conditions, staining is less well-defined and cell-cell interfaces cannot be delineated. Scale bar = 50 μm. *B*: quantification of occludin staining as expressed by % of positive pixels per cell number. **$P < 0.01$.

We first characterized and optimized the epithelial mucociliary transport function of a previously developed in vitro model of the airway wall that can undergo lateral dynamic compression (12). The utility of previously developed in vitro models for studying transepithelial transport-related phenomena is limited by the level of bronchial epithelial cell differentiation and ciliary function attainable (10–12, 50, 51, 55). Culture conditions that were previously developed to promote epithelial differentiation towards a pseudostratified state include coculture with fibroblasts within a 3D matrix (1, 11, 50, 51, 63, 64, 75), the addition of specific factors to a serum-free media (15, 27, 55), and culture in ALI after epithelial cells have reached confluence (3, 15, 18, 49, 65). We further optimized the medium composition for ciliogenesis and cultured for 21 days at ALI. The culture conditions presented here showed more physiological ciliogenesis, both in length and percent coverage. Furthermore, we observed particle trajectories that extended

across several cells, suggesting some degree of coordination between cells. However, we observed a high variability both in the transport velocities and in the type of motion of particles on the epithelium. In actual bronchi, cilia sweep upward to remove debris from the lungs, but since our model was symmetric in the *x* and *y* directions (without strain) we did not expect an overall directionality. The effects of dynamic strain on ciliary motion were not considered in this work, although it has been previously shown that mechanical stimulation leads to intra- and intercellular Ca^{2+} signaling that would increase ciliary beat frequency (5, 56, 66). Therefore, the increase in overall infection rate that we see is unlikely to be due to any changes in ciliary beat frequency or coordination. Instead, considering that mechanical compression causes buckling of the epithelium and mucosal folding, a virus could accumulate in the folds and transmigrate through the areas of damaged epithelium with an increased rate due to epithelial damage strain-enhanced transport.

To ponder the physiological relevance of the strain we applied to our in vitro models, we first considered that the strain magnitude within any bronchoconstricted airway wall is highly nonuniform; SMCs on the outer perimeter shorten to cause compression of the airway wall (25), but since the internal perimeter remains constant (maintained by the basement membrane), the epithelium buckles into the lumen (34, 40, 58, 74). Furthermore, strain varies radially from the epithelium to the subepithelium due to geometry, buckling, and different mechanical properties of epithelial vs. subepithelial regions. Finally, strain profiles are different in bronchoconstricted airways of normal vs. asthmatic patients, because of the mechanics and increased thickness of the remodeled airway wall (35, 53, 54, 74) as well as increased contractile forces of asthmatic SMCs (8, 25, 57). A number of studies (29, 30, 32, 34, 47, 58) have shown that in models of induced (e.g., by methacholine or histamine) bronchoconstriction, the maximum level of SMC shortening (i.e., that which causes complete closure of the lumen) is 30–40%. These maximal levels of SMC or outer wall strain were induced in normal subjects, whereas asthmatic airways have thicker and stiffer lamina propria and submucosal layers; we therefore expect maximum compressive strains (but not necessarily stresses) in the asthmatic airway wall to be considerably <30%. Thus, it is reasonable to assume that 15% strain applied laterally to a rectangular model of the airway wall is a reasonable mimic of in vivo bronchoconstriction. As to the strain rate, bronchoconstriction occurs intermittently in vivo and can last from seconds to minutes (43) and thus our applied rate of 0.1 Hz was used to test the effects of a relatively slow compression and relaxation of the airway all model on a relevant timescale.

The model virus we used constitutes a well-characterized lentiviral system that is relatively easy to track, since the virus itself is not fluorescent but an infected cell will become fluorescent after expressing the GFP transgene. The transduction efficiency of target cells depends partially on the type of glycoprotein used to coat retroviral vectors, since this influences the mechanism by which the virus enters the cell. The envelope we used to coat the virus is widely used due to its efficiency in entering most cell types: its receptor is thought to be a lipid component of the cell plasma membrane (LBPA) that is widely distributed on the surface of most cell types (69), and it is thought to enter the cell by receptor-mediated endocytosis.

It is commonly believed that a lentivirus with a VSV-G envelope most efficiently enters from the basal side of airway epithelial cells, although some studies (6, 37–39, 59, 72) show efficient apical infection. Since we introduced lentivirus originally on the apical surface of the epithelium, we can hypothesize that, in our model, mechanical stress either enhances the expression of the VSV-G receptor on the apical side or it enhances the access of the virus to the basal side through epithelial damage and/or enhanced transepithelial transport. The fact that subepithelial fibroblasts were more frequently infected under mechanical stress suggests that convection played an important role, particularly considering that virus transport is critical for cell infection (since in this system an infected cell cannot infect another cell; only the free virus can infect another cell).

In conclusion, using an in vitro model of the airway wall with relevant epithelial barrier functions, we showed that cell infection by lentivirus applied on the apical surface of the mucosa is strongly enhanced by dynamic compressive strain of 15% at 0.1 Hz. The strain increased both the percentage of airway epithelial cells infected as well as that of subepithelial fibroblasts. This not only highlights the mechanical environment of the airways as an important factor in viral infection susceptibility but also suggests that dynamic mechanical stress may be an important design strategy in viral therapies aimed at delivering transgenes to cells of the airway wall.

REFERENCES

1. **Agarwal A, Coleno ML, Wallace VP, Wu WY, Sun CH, Tromberg BJ, George SC.** Two-photon laser scanning microscopy of epithelial cell-modulated collagen density in engineered human lung tissue. *Tissue Eng* 7: 191–202, 2001.
2. **Akinbami LJ, Schoendorf KC.** Trends in childhood asthma: prevalence, health care utilization, and mortality. *Pediatrics* 110: 315–322, 2002.
3. **Beckmann JD, Takizawa H, Romberger D, Illig M, Claassen L, Rickard K, Rennard SI.** Serum-free culture of fractionated bovine bronchial epithelial cells. *In Vitro Cell Dev Biol* 28A: 39–46, 1992.
4. **Bianco A, Whiteman SC, Sethi SK, Allen JT, Knight RA, Spiteri MA.** Expression of intercellular adhesion molecule-1 (ICAM-1) in nasal epithelial cells of atopic subjects: a mechanism for increased rhinovirus infection? *Clin Exp Immunol* 121: 339–345, 2000.
5. **Boitano S, Dirksen ER, Sanderson MJ.** Intercellular propagation of calcium waves mediated by inositol trisphosphate. *Science* 258: 292–295, 1992.
6. **Borok Z, Harboe-Schmidt JE, Brody SL, You Y, Zhou B, Li X, Cannon PM, Kim KJ, Crandall ED, Kasahara N.** Vesicular stomatitis virus G-pseudotyped lentivirus vectors mediate efficient apical transduction of polarized quiescent primary alveolar epithelial cells. *J Virol* 75: 11747–11754, 2001.
7. **Bousquet J, Jeffery PK, Busse WW, Johnson M, Vignola AM.** Asthma. From bronchoconstriction to airways inflammation and remodeling. *Am J Respir Crit Care Med* 161: 1720–1745, 2000.
8. **Brown RH, Georgakopoulos J, Mitzner W.** Individual canine airways responsiveness to aerosol histamine and methacholine in vivo. *Am J Respir Crit Care Med* 157: 491–497, 1998.
9. **Busse WW, Gern JE.** Viruses in asthma. *J Allergy Clin Immunol* 100: 147–150, 1997.
10. **Chakir J, Page N, Hamid Q, Laviolette M, Boulet LP, Rouabhia M.** Bronchial mucosa produced by tissue engineering: a new tool to study cellular interactions in asthma. *J Allergy Clin Immunol* 107: 36–40, 2001.
11. **Choe MM, Sporn PH, Swartz MA.** Extracellular matrix remodeling by dynamic strain in a three-dimensional tissue-engineered human airway wall model. *Am J Respir Cell Mol Biol* 35: 306–313, 2006.
12. **Choe MM, Sporn PH, Swartz MA.** An in vitro airway wall model of remodeling. *Am J Physiol Lung Cell Mol Physiol* 285: L427–L433, 2003.
13. **Choe MM, Tomei AA, Swartz MA.** Physiological 3D tissue model of the airway wall and mucosa. *Nat Protoc* 1: 357–362, 2006.
14. **Chu EK, Foley JS, Cheng J, Patel AS, Drazen JM, Tschumperlin DJ.** Bronchial epithelial compression regulates epidermal growth factor receptor family ligand expression in an autocrine manner. *Am J Respir Cell Mol Biol* 32: 373–380, 2005.
15. **Clark AB, Randell SH, Nettesheim P, Gray TE, Bagnell B, Ostrowski LE.** Regulation of ciliated cell differentiation in cultures of rat tracheal epithelial cells. *Am J Respir Cell Mol Biol* 12: 329–338, 1995.
16. **Cohn L, Elias JA, Chupp GL.** Asthma: mechanisms of disease persistence and progression. *Annu Rev Immunol* 22: 789–815, 2004.
17. **Davies DE, Wicks J, Powell RM, Puddicombe SM, Holgate ST.** Airway remodeling in asthma: new insights. *J Allergy Clin Immunol* 111: 215–225, 2003.
18. **de Jong PM, van Sterkenburg MA, Hesseling SC, Kempenaar JA, Mulder AA, Mommaas AM, Dijkman JH, Ponec M.** Ciliogenesis in human bronchial epithelial cells cultured at the air-liquid interface. *Am J Respir Cell Mol Biol* 10: 271–277, 1994.
19. **Djukanovic R.** Asthma: a disease of inflammation and repair. *J Allergy Clin Immunol* 105: S522–526, 2000.
20. **Ehrhardt C, Collnot EM, Baldes C, Becker U, Laue M, Kim KJ, Lehr CM.** Towards an in vitro model of cystic fibrosis small airway epithelium: characterisation of the human bronchial epithelial cell line CFBE41o. *Cell Tissue Res* 323: 405–415, 2006.
21. **Fahy JV, Corry DB, Boushey HA.** Airway inflammation and remodeling in asthma. *Curr Opin Pulm Med* 6: 15–20, 2000.
22. **Ferdousi HA, Zetterstrom O, Dreborg S.** Bronchial hyper-responsiveness predicts the development of mild clinical asthma within 2 yr in school children with hay-fever. *Pediatr Allergy Immunol* 16: 478–486, 2005.
23. **Fireman P.** Understanding asthma pathophysiology. *Allergy Asthma Proc* 24: 79–83, 2003.
24. **Fredberg JJ.** Airway obstruction in asthma: does the response to a deep inspiration matter? *Respir Res* 2: 273–275, 2001.
25. **Fredberg JJ.** Bronchospasm and its biophysical basis in airway smooth muscle. *Respir Res* 5: 2, 2004.
26. **Gern JE, Busse WW.** Association of rhinovirus infections with asthma. *Clin Microbiol Rev* 12: 9–18, 1999.
27. **Gray TE, Guzman K, Davis CW, Abdullah LH, Nettesheim P.** Mucociliary differentiation of serially passaged normal human tracheobronchial epithelial cells. *Am J Respir Cell Mol Biol* 14: 104–112, 1996.
28. **Griffith LG, Swartz MA.** Capturing complex 3D tissue physiology in vitro. *Nat Rev Mol Cell Biol* 7: 211–224, 2006.
29. **Gunst SJ, Stropp JQ.** Pressure-volume and length-stress relationships in canine bronchi in vitro. *J Appl Physiol* 64: 2522–2531, 1988.
30. **Hahn HL, Graf PD, Nadel JA.** Effect of vagal tone on airway diameters and on lung volume in anesthetized dogs. *J Appl Physiol* 41: 581–589, 1976.
31. **Hasaneen NA, Zucker S, Cao J, Chiarelli C, Panettieri RA, Foda HD.** Cyclic mechanical strain-induced proliferation and migration of human airway smooth muscle cells: role of EMMPRIN and MMPs. *FASEB J* 19: 1507–1509, 2005.
32. **Hulbert WC, McLean T, Wiggs B, Pare PD, Hogg JC.** Histamine dose-response curves in guinea pigs. *J Appl Physiol* 58: 625–634, 1985.
33. **James A.** Airway remodeling in asthma. *Curr Opin Pulm Med* 11: 1–6, 2005.
34. **James AL, Hogg JC, Dunn LA, Pare PD.** The use of the internal perimeter to compare airway size and to calculate smooth muscle shortening. *Am Rev Respir Dis* 138: 136–139, 1988.
35. **Jeffery PK, Godfrey RW, Adelroth E, Nelson F, Rogers A, Johansson SA.** Effects of treatment on airway inflammation and thickening of basement membrane reticular collagen in asthma. A quantitative light and electron microscopic study. *Am Rev Respir Dis* 145: 890–899, 1992.
36. **Johnston SL, Pattemore PK, Sanderson G, Smith S, Campbell MJ, Josephs LK, Cunningham A, Robinson BS, Myint SH, Ward ME, Tyrrell DA, Holgate ST.** The relationship between upper respiratory infections and hospital admissions for asthma: a time-trend analysis. *Am J Respir Crit Care Med* 154: 654–660, 1996.
37. **Kang Y, Stein CS, Heth JA, Sinn PL, Penisten AK, Staber PD, Ratliff KL, Shen H, Barker CK, Martins I, Sharkey CM, Sanders DA, McCray PB Jr, Davidson BL.** In vivo gene transfer using a nonprimate lentiviral vector pseudotyped with Ross River virus glycoproteins. *J Virol* 76: 9378–9388, 2002.

38. **Kobayashi M, Iida A, Ueda Y, Hasegawa M.** Pseudotyped lentivirus vectors derived from simian immunodeficiency virus SIVagm with envelope glycoproteins from paramyxovirus. *J Virol* 77: 2607–2614, 2003.

39. **Kobinger GP, Weiner DJ, Yu QC, Wilson JM.** Filovirus-pseudotyped lentiviral vector can efficiently and stably transduce airway epithelia in vivo. *Nat Biotechnol* 19: 225–230, 2001.

40. **Lambert RK.** Role of bronchial basement membrane in airway collapse. *J Appl Physiol* 71: 666–673, 1991.

41. **Lambert RK, Codd SL, Alley MR, Pack RJ.** Physical determinants of bronchial mucosal folding. *J Appl Physiol* 77: 1206–1216, 1994.

42. **Le Bellego F, Plante S, Chakir J, Hamid Q, Ludwig MS.** Differences in MAP kinase phosphorylation in response to mechanical strain in asthmatic fibroblasts. *Respir Res* 7: 68, 2006.

43. **Lee P, Abisheganaden J, Chee CB, Wang YT.** A new asthma severity index: a predictor of near-fatal asthma? *Eur Respir J* 18: 272–278, 2001.

44. **Lin H, Li H, Cho HJ, Bian S, Roh HJ, Lee MK, Kim JS, Chung SJ, Shim CK, Kim DD.** Air-liquid interface (ALI) culture of human bronchial epithelial cell monolayers as an in vitro model for airway drug transport studies. *J Pharm Sci* 96: 341–350, 2007.

45. **Matsui H, Randell SH, Peretti SW, Davis CW, Boucher RC.** Coordinated clearance of periciliary liquid and mucus from airway surfaces. *J Clin Invest* 102: 1125–1131, 1998.

46. **Mellow TE, Murphy PC, Carson JL, Noah TL, Zhang L, Pickles RJ.** The effect of respiratory synctial virus on chemokine release by differentiated airway epithelium. *Exp Lung Res* 30: 43–57, 2004.

47. **Moreno RH, Hogg JC, Pare PD.** Mechanics of airway narrowing. *Am Rev Respir Dis* 133: 1171–1180, 1986.

48. **Munakata M.** Airway remodeling and airway smooth muscle in asthma. *Allergy* 55: 235–243, 2006.

49. **Neugebauer P, Endepols H, Mickenhagen A, Walger M.** Ciliogenesis in submersion and suspension cultures of human nasal epithelial cells. *Eur Arch Otorhinolaryngol* 260: 325–330, 2003.

50. **Paquette JS, Moulin V, Tremblay P, Bernier V, Boutet M, Laviolette M, Auger FA, Boulet LP, Goulet F.** Tissue-engineered human asthmatic bronchial equivalents. *Eur Cell Mater* 7: 1–11, 2004.

51. **Paquette JS, Tremblay P, Bernier V, Auger FA, Laviolette M, Germain L, Boutet M, Boulet LP, Goulet F.** Production of tissue-engineered three-dimensional human bronchial models. *In Vitro Cell Dev Biol Anim* 39: 213–220, 2003.

52. **Ressler B, Lee RT, Randell SH, Drazen JM, Kamm RD.** Molecular responses of rat tracheal epithelial cells to transmembrane pressure. *Am J Physiol Lung Cell Mol Physiol* 278: L1264–L1272, 2000.

53. **Roberts CR.** Is asthma a fibrotic disease? *Chest* 107: 111S–117S, 1995.

54. **Roche WR, Beasley R, Williams JH, Holgate ST.** Subepithelial fibrosis in the bronchi of asthmatics. *Lancet* 1: 520–524, 1989.

55. **Sachs LA, Finkbeiner WE, Widdicombe JH, de Jong PM, van Sterkenburg MA, Hesseling SC, Kempenaar JA, Mulder AA, Mommaas AM, Dijkman JH, Ponec M.** Effects of media on differentiation of cultured human tracheal epithelium. *In Vitro Cell Dev Biol Anim* 39: 56–62, 2003.

56. **Sanderson MJ, Charles AC, Dirksen ER.** Mechanical stimulation and intercellular communication increases intracellular Ca^{2+} in epithelial cells. *Cell Regul* 1: 585–596, 1990.

57. **Seow CY, Schellenberg RR, Pare PD.** Structural and functional changes in the airway smooth muscle of asthmatic subjects. *Am J Respir Crit Care Med* 158: S179–186, 1998.

58. **Seow CY, Wang L, Pare PD.** Airway narrowing and internal structural constraints. *J Appl Physiol* 88: 527–533, 2000.

59. **Sinn PL, Penisten AK, Burnight ER, Hickey MA, Williams G, McCoy DM, Mallampalli RK, McCray PB.** Gene transfer to respiratory epithelia with lentivirus pseudotyped with Jaagsiekte sheep retrovirus envelope glycoprotein. *Hum Gene Ther* 16: 479–488, 2005.

60. **Swartz MA, Tschumperlin DJ, Kamm RD, Drazen JM.** Mechanical stress is communicated between different cell types to elicit matrix remodeling. *Proc Natl Acad Sci USA* 98: 6180–6185, 2001.

61. **Tanihara S, Nakamura Y, Oki I, Ojima T, Yanagawa H.** Trends in asthma morbidity and mortality in Japan between 1984 and 1996. *J Epidemiol* 12: 217–222, 2002.

62. **Terajima M, Yamaya M, Sekizawa K, Okinaga S, Suzuki T, Yamada N, Nakayama K, Ohrui T, Oshima T, Numazaki Y, Sasaki H.** Rhinovirus infection of primary cultures of human tracheal epithelium: role of ICAM-1 and IL-1β. *Am J Physiol Lung Cell Mol Physiol* 273: L749–L759, 1997.

63. **Thompson HG, Mih JD, Krasieva TB, Tromberg BJ, George SC.** Epithelial-derived TGF-β2 modulates basal and wound-healing subepithelial matrix homeostasis. *Am J Physiol Lung Cell Mol Physiol* 291: L1277–L1285, 2006.

64. **Thompson HG, Truong DT, Griffith CK, George SC.** A three-dimensional in vitro model of angiogenesis in the airway mucosa. *Pulm Pharmacol* 20: 141–148, 2007.

65. **Thornton DJ, Gray T, Nettesheim P, Howard M, Koo JS, Sheehan JK.** Characterization of mucins from cultured normal human tracheobronchial epithelial cells. *Am J Physiol Lung Cell Mol Physiol* 278: L1118–L1128, 2000.

66. **Tschumperlin DJ, Drazen JM.** Chronic effects of mechanical force on airways. *Annu Rev Physiol* 68: 563–583, 2006.

67. **Tschumperlin DJ, Shively JD, Kikuchi T, Drazen JM.** Mechanical stress triggers selective release of fibrotic mediators from bronchial epithelium. *Am J Respir Cell Mol Biol* 28: 142–149, 2003.

68. **Tschumperlin DJ, Shively JD, Swartz MA, Silverman ES, Haley KJ, Raab G, Drazen JM.** Mechanotransduction in the lung - Bronchial epithelial compression regulates MAP kinase signaling and HB-EGF-like growth factor expression. *Am J Physiol Lung Cell Mol Physiol* 282: L904–L911, 2002.

69. **Uchil P, Mothes W.** Viral entry: a detour through multivesicular bodies. *Nat Cell Biol* 7: 641–642, 2005.

70. **Vignola AM, Mirabella F, Costanzo G, Di Giorgi R, Gjomarkaj M, Bellia V, Bonsignore G.** Airway remodeling in asthma. *Chest* 123: 417S-422S, 2003.

71. **Wadsworth SJ, Nijmeh HS, Hall IP.** Glucocorticoids increase repair potential in a novel in vitro human airway epithelial wounding model. *J Clin Immunol* 26: 376–387, 2006.

72. **Wang G, Slepushkin V, Zabner J, Keshavjee S, Johnston JC, Sauter SL, Jolly DJ, Dubensky TW Jr, Davidson BL, McCray PB Jr.** Feline immunodeficiency virus vectors persistently transduce nondividing airway epithelia and correct the cystic fibrosis defect. *J Clin Invest* 104: R55–62, 1999.

73. **Waters CM, Sporn PH, Liu M, Fredberg JJ.** Cellular biomechanics in the lung. *Am J Physiol Lung Cell Mol Physiol* 283: L503–L509, 2002.

74. **Wiggs BR, Hrousis CA, Drazen JM, Kamm RD.** On the mechanism of mucosal folding in normal and asthmatic airways. *J Appl Physiol* 83: 1814–1821, 1997.

75. **Zhang S, Smartt H, Holgate ST, Roche WR.** Growth factors secreted by bronchial epithelial cells control myofibroblast proliferation: an in vitro coculture model of airway remodeling in asthma. *Lab Invest* 79: 395–405, 1999.